Radially and azimuthally polarized beams generated by space-variant dielectric subwavelength gratings

Ze'ev Bomzon, Gabriel Biener, Vladimir Kleiner, and Erez Hasman

Optical Engineering Laboratory, Faculty of Mechanical Engineering, Technion—Israel Institute of Technology, Haifa 32000, Israel

Received August 16, 2001

We present a novel method for forming radially and azimuthally polarized beams by using computer-generated subwavelength dielectric gratings. The elements were deposited upon GaAs substrates and produced beams with a polarization purity of 99.2% at a wavelength of 10.6 μm. We have verified the polarization properties with full space-variant polarization analysis and measurement, and we show that such beams have certain vortexlike properties and that they carry angular momentum. © 2002 Optical Society of America

OCIS codes: 260.5430, 050.1950, 050.2770, 230.5440.

Singularities in optical fields have received much attention lately.[1] Such singularities appear at points or lines where the phase or the amplitude of the wave is undefined or changes abruptly. One class of dislocation is vortices, which are spiral phase ramps about a singularity. Vortices are characterized by a topological charge, $l = (1/2\pi) \oint \nabla\varphi \, ds$, where φ is the phase of the beam and l is an integer. Until now, research had focused mainly on field dislocations in scalar waves. However, if we allow for the polarization to be space varying (i.e., transversely inhomogeneous), disclinations can arise.[2] Disclinations are points or lines of singularity in the patterns or directions of a transverse field. An example is the center of a beam with radial or azimuthal polarization. Such beams can be created by interferometry,[3] by intracavity summation of two beams,[4] or by use of space-variant metal stripe gratings.[5] However, all these methods are somewhat cumbersome, are unstable, or have low efficiency.

In this Letter we present a method for using computer-generated space-variant subwavelength dielectric gratings for the formation of radially and azimuthally polarized light. By correctly determining the direction, period, and depth of the grating, one can obtain any desired continuous polarization. Furthermore, the continuity of our grating ensures the continuity of the transmitted field, thus suppressing diffraction effects that may arise from discontinuity. Our gratings are compact, lightweight, and flexible in design and have high transmission efficiency. We discuss the design and fabrication processes and show that the gratings can cause disclinations. We also demonstrate that one can define a topological charge for these beams and that it is related to the beams' angular momentum. We analyze their propagation by using scalar vortex theory. We substantiate our conclusions by presenting experimental results obtained with CO_2 laser radiation at a wavelength of 10.6 μm.

Space-variant subwavelength gratings are typically described by a grating vector,

$$\mathbf{K}_g = K_0(r,\theta)\{\cos[\beta(\theta,r)]\hat{r} + \sin[\beta(\theta,r)]\hat{\theta}\}, \qquad (1)$$

where $\hat{r}$ and $\hat{\theta}$ are unit vectors in polar coordinates, $K_0 = 2\pi/\Lambda(r,\theta)$ is the local spatial frequency for a grating of local period $\Lambda(r,\theta)$, and $\beta(r,\theta)$ is the local direction of the vector, chosen such that it is perpendicular to the grating stripes. When the period of the grating is smaller than the incident wavelength, only the zeroth order is a propagating order, and such gratings behave as layers of a uniaxial crystal with the optical axes perpendicular and parallel to the grating grooves.[6] The effective birefringence of these gratings depends on their structure, and therefore by correctly controlling the structure one can create any desired wave plate.

Assume that we wish to construct a grating for converting right-hand circularly polarized light into radial polarization. We can do this by using a space-varying quarter-wave plate; i.e., the depth and structure of the local grating are such that the retardation is $\pi/2$. In addition we need to require that $\beta = -45°$ at all points to ensure that the resultant polarization is linearly polarized in the desired direction. (Note that incident left-hand circular polarization will result in an azimuthally polarized beam.) Applying β to Eq. (1) and ensuring the continuity of the grating by requiring that $\nabla \times \mathbf{K}_g = 0$ result in

$$\frac{1}{r}\left\{\frac{\partial}{\partial r}[rK_0(r,\theta)] + \frac{\partial K_0(r,\theta)}{\partial\theta}\right\} = 0. \qquad (2)$$

Owing to the symmetry of the problem we may assume that K_0 is independent of θ, in which case Eq. (2) can be solved to yield $K_0(r) = (2\pi r_0/\Lambda_0)(1/r)$, where Λ_0 is the period when $r = r_0$. Integrating the resultant vector along an arbitrary path yields the grating function (defined such that $\nabla\phi = \mathbf{K}_g$)

$$\phi = (2\pi r_0/\sqrt{2}\,\Lambda_0)[\ln(r/r_0) - \theta]. \qquad (3)$$

Continuity of this function requires that $\phi(r,\theta) = \phi(r,\theta + 2\pi) \pm 2\pi m$ (m is an integer), and therefore $2\pi r_0/\sqrt{2}\,\Lambda_0$ must be an integer, placing a constraint on r_0 and Λ_0.

We fabricated a Lee-type binary grating described by the function of Eq. (3). The grating had the values $\Lambda_0 = 2$ μm and $r_0 = 5$ mm, such that 5 mm $< r <$ 8 mm, and 2 μm $< \Lambda <$ 3.2 μm, such as not to exceed the Wood anomaly. First we fabricated

0146-9592/02/050285-03$15.00/0

a chrome mask of the grating, using high-resolution laser lithography. The pattern was transferred by photolithography to a 500-μm-thick GaAs wafer, after which we etched the grating by using electron cyclotron resonance with BCl_3 for 39 min. Finally, we applied an antireflection coating to the back side of the wafer. Figure 1(a) shows the geometry of this grating as well as a typical cross section of the grating profile taken with a scanning-electron microscope. We note the intricate structure of the grating and the smooth and well-defined profile of the grooves. We used this image to measure the grating profile for simulations with rigorous coupled-wave analysis.[7] The simulations showed that the retardation at the relevant periods was close to $\pi/2$. We confirmed this experimentally with a chirped grating whose period varied linearly over the relevant range.

Following the fabrication we illuminated the grating with right-hand circular polarized light, imaged it onto a Spiricon Pyrocam I infrared camera, and measured the Stokes parameters (S_0–S_3) at each point by using the four-measurement technique.[8] We then calculated the local azimuthal angle, ψ, and ellipticity, $\tan(\chi)$, of the beam as $\tan(2\psi) = S_2/S_1$ and $\sin(2\chi) = S_3/S_0$, respectively. We found an average ellipticity of $\tan(\chi) = 0.08$ and an average deviation of the azimuthal angle of 2.6°, yielding a polarization purity (percentage of energy in the desired polarization) of 99.2%. We also found a transmission of 86%, which we verified with rigorous coupled-wave analysis, using the grating profile from Fig. 1. Figure 1(b) shows the local azimuthal angle of the resultant beam, and the arrows show the radial polarization. Figure 1(c) shows the resultant local azimuthal angle when the incident beam has left-hand circular polarization, and we can see the azimuthally polarized beam as predicted. Thus the single element can be used to form either radial or azimuthal polarization.

We gained additional insight by performing a theoretical full space-variant polarization and phase analysis of the element. By representing the element as a space-variant Jones matrix, one can find the resultant wave front for any incident polarization.[5] This analysis showed that, for a space-varying quarter-wave plate and incident circular polarization, the Jones vector of the resultant beam will be

$$\mathbf{E} = (\cos\,\theta,\ \sin\,\theta)^T\ \exp(-i\theta)\,. \tag{4}$$

From here we can calculate the space-variant Pancharatnam phase[9] (based on the rule proposed by Pancharatnam for comparing the phases of two light beams in different states of polarization) of the transmitted beam as $\varphi_p(r,\,\theta) = \arg\langle \mathbf{E}(r,\,\theta), \mathbf{E}(R,\,0)\rangle$, where $\arg\langle \mathbf{E}_1, \mathbf{E}_2\rangle$ is the argument of the inner product of two Jones vectors and $(R,\,0)$ are the radial coordinates of the point on the resultant beam, relative to which the phase is measured. This calculation yields $\varphi_p(\theta) = \arg[\cos\,\theta\,\exp(-i\theta)]$.

The beam displays a Pancharatnam phase ramp similar to those found in vortices, and we therefore define the topological Pancharatnam charge as $l_p = (1/2\pi)\oint \nabla\varphi_p ds - 1$. Note that 1 is the singularity index of the disclination, i.e., the number of times that the azimuthal angle rotates about the disclination.[2] (It is also half of the number of discontinuities of φ_p in a cycle about the disclination). The calculation yields a topological Pancharatnam charge of $l_p = +1$ for the wave in Eq. (4). This charge can be modified by transmission of the beam through a spiral phase plate of the form $\exp(il_d\theta)$ (l_d is an integer), in which case a topological Pancharatnam charge of l_d is added to the beam. Note that l_d is exactly equal to the topological charge associated with the phase plate.

Figure 2 shows the calculated real part of the instantaneous fields of radially polarized beams. Figure 2(a) shows the field of the beam that is formed by use of the grating only. Figures 2(b), 2(c), 2(d), and 2(e) show the beam that is created when, in addition to the grating, the wave is also transmitted through spiral phase elements of the forms $\exp(i\theta)$, $\exp(-i\theta)$, $\exp(i2\theta)$, and $\exp(-i2\theta)$, respectively. We note that the beams of Figs. 2(a) and 2(d) have the same form. In addition, the absolute value of their topological Pancharatnam charge is the same (although of opposite sign), hinting that the beams display similar characteristics.

Figure 3 shows the far-field images of these fields in their respective order [e.g., Fig. 3(a) corresponds to Fig. 2(a), Fig. 3(b) corresponds to Fig. 2(b)] as well as the theoretically calculated cross sections. We note that Figs. 3(a) and 3(d) exhibit the same far-field image with a bright center, as expected, whereas the beams in Figs. 3(b)–3(e) exhibit distinct far-field images with dark centers.

We can explain these images by expressing the beams as the coherent sum of two orthogonally polarized components with circular polarization. The beam of Fig. 3(a), which is described in Eq. (4), can then be rewritten as

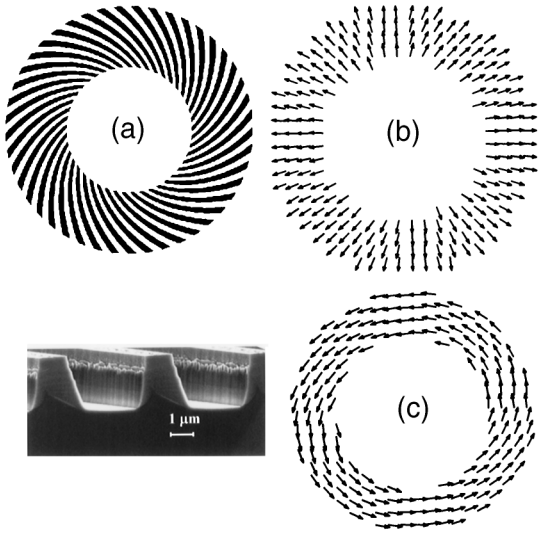

Fig. 1. (a) Geometry of the space-variant grating as well as an image of a typical grating profile taken with a scanning-electron microscope. The experimentally measured local azimuthal angles of the beam when the incident polarization is (b) right-hand circular and (c) left-hand circular are also shown.

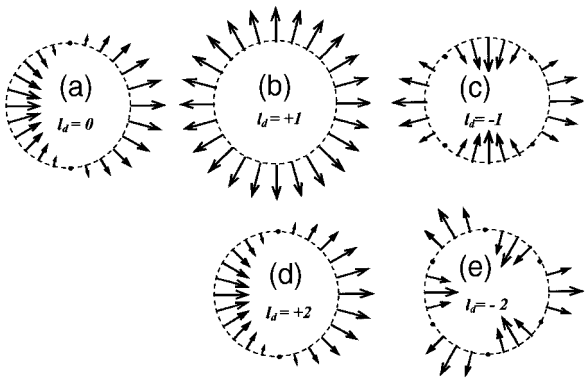

Fig. 2. Calculated real part of the instantaneous vector fields for the radial polarization formed (a) by the grating and (b)–(e) with additional spiral phase plates as shown.

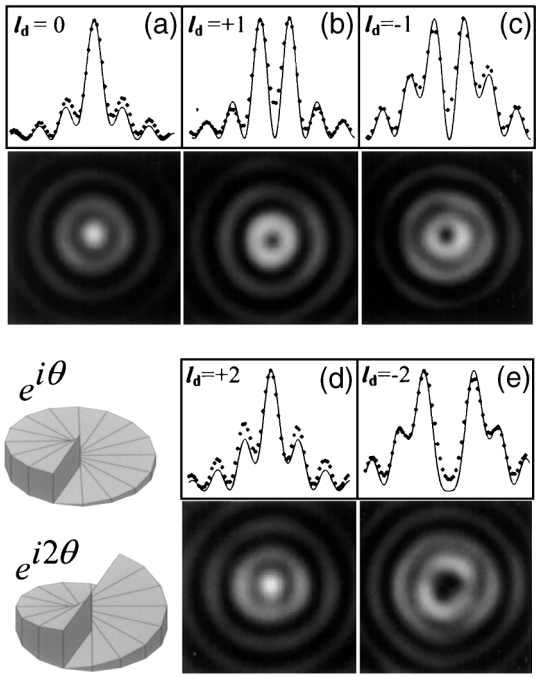

Fig. 3. Experimental far-field images for the beams in Fig. 2 as well as their calculated and measured cross sections. The geometry of the spiral phase plates is shown at the bottom left.

$$\mathbf{E} = 1/2[(1, i)^T \exp(-i2\theta) + (1, -i)^T]. \quad (5)$$

We can find all the other beams by multiplying each of the components by $\exp(il_d\theta)$. In Eq. (5) the beam consists of a scalar wave with topological charge -2 and a wave with 0 topological charge. The wave with charge -2 conserves its vortex, whereas the wave with 0 charge collapses and causes the bright center. When we apply the same logic to the wave of Fig. 3(b), we find that that wave consists of two scalar vortices, with topological charges -1 and $+1$. Neither of the two vortices collapses, and the dark spot is retained. The beams of Figs. 3(c)–3(e) can be analyzed in the same fashion.

Another point of interest is the angular momentum of these beams. For a scalar wave, the angular momentum in the direction of propagation per unit energy is $J_z = (l + \sigma)/\omega$,[10] where l is the topological charge, σ is the helicity (± 1 for circular polarization), and ω is the optical frequency of the wave front. Using this rule and the decomposition presented in Eq. (5), we found that radially polarized beams carry an angular momentum of

$$J_z = \left[\frac{1}{2}\sum_{i=L,R}(\sigma_i + l_i)\right] \Big/ \omega = l_p/\omega$$
$$= \left(\frac{1}{2\pi}\oint \nabla\varphi_p \mathrm{d}s - 1\right) \Big/ \omega,$$

where L and R indicate the components with left and right circular polarization, respectively, and that the angular momentum of these waves is given by the topological Pancharatnam charge. The same results hold for any beam with axially symmetric linear polarization[11] with 1 replaced by the appropriate singularity index. Our results show a connection between angular momentum and topological Pancharatnam charge. The nature of that connection is still unclear and requires additional investigation.

Z. Bomzon's e-mail address is zbomzy@tx.technion.ac.il.

References

1. G. A. Swartzlander, Jr., Opt. Lett. **26,** 497 (2001).
2. J. F. Nye, Proc. R. Soc. London Ser. A **387,** 105 (1983).
3. S. Tidwell, G. H. Kim, and W. D. Kimura, Appl. Opt. **32,** 5222 (1993).
4. R. Oron, S. Blit, N. Davidson, A. A. Friesem, Z. Bomzon, and E. Hasman, Appl. Phys. Lett. **77,** 3322 (2000).
5. Z. Bomzon, V. Kleiner, and E. Hasman, Opt. Lett. **26,** 1424 (2001).
6. A. G. Lopez and H. G. Craighead, Opt. Lett. **23,** 1627 (1998).
7. M. G. Moharam and T. K. Gaylord, J. Opt. Soc. Am. A **3,** 1780 (1986).
8. E. Collet, *Polarized Light* (Marcel Dekker, New York, 1993).
9. S. Pancharatnam, Proc. Ind. Acad. Sci. **44,** 247 (1956).
10. L. Allen, M. J. Padgett, and M. Babiker, in *Progress in Optics*, E. Wolf, ed. (Elsevier, Amsterdam, 1999), Vol. XXXIX, pp. 291–370.
11. M. Stalder and M. Schadt, Opt. Lett. **21,** 1948 (1996).